

# RESEARCH AND SIMULATION ANALYSIS OF PEANUT COMBINED HARVESTER EXCAVATING DEVICE

## 花生联合收获机挖掘装置研究与仿真分析

Baiqiang ZUO<sup>1)</sup>, Shuqi SHANG<sup>1)</sup>, Xiaoning HE<sup>1)</sup>, Zenghui GAO<sup>2)</sup>, Wei LIU<sup>3)</sup>, Chunxiao ZHANG<sup>1)</sup>, Zhenjia MA<sup>1)</sup>, Dongwei WANG<sup>\*1)</sup>

<sup>1)</sup> Qingdao Agricultural University, College of Mechanical and Electrical Engineering / China;

<sup>2)</sup> Xinjiang Agricultural University, College of Mechanical and Electrical Engineering / China;

<sup>3)</sup> Shandong Yuanquan Mechanical Co / China

Tel: +86-0532-58957391; E-mail: 200701031@qau.edu.cn

DOI: <https://doi.org/10.35633/inmateh-68-38>

**Keywords:** peanut combine harvester, digging shovel, optimization, simulation analysis, experiment

### ABSTRACT

For the peanut combine harvester excavation process resistance, poor soil crushing effect and poor reliability of the problem, the excavation shovel optimization needs improvement. Firstly, a mechanical model of the resistance of the excavation shovel was established to investigate the key factors affecting the degree of resistance of the excavation shovel. Next, the design of the main parameters of the excavation shovel was done to determine the range of values of the main factors affecting the peanut excavation shovel. EDEM software was used to simulate and analyse the excavation process and to explore the influence law of excavation shovel parameters on the resistance. Improvements were made to the excavation shovel, discrete element simulation tests were used to demonstrate that the optimized excavation device had better resistance reduction and soil crushing than the original device. By designing a three-factor, three-level orthogonal simulation test, the best parameters for the excavation shovel were obtained: the shovel surface inclination is 20°, the excavation depth is 131mm, and the shovel surface width is 277mm. Field trials were conducted under the optimal combination of parameters to test the reliability of the improved digging shovel. Compared with the operating effectiveness of the original machine, the result was improved to some extent. It proves that the optimized design of excavating shovel is reasonable and can improve the operation effect of peanut harvester.

### 摘要

针对花生联合收获机存在挖掘作业过程阻力大、碎土作业效果差以及可靠性差的问题，对挖掘铲进行优化改进。首先建立挖掘铲阻力力学模型，探究影响挖掘铲阻力大小的关键因素。其次对挖掘铲的主要参数进行设计，确定影响花生挖掘铲的主要因素取值范围。利用EDEM软件对挖掘过程进行仿真分析，探明挖掘铲参数对阻力的影响规律。对挖掘铲进行改进，利用离散元仿真试验证明了优化后的挖掘装置的减阻和破碎土壤效果优于原装置。通过设计三因素三水平正交仿真试验，得出挖掘铲最佳的参数组合：铲面倾角为20°，挖掘深度为131mm，铲面宽度为277mm。在最优参数组合下进行田间试验，检验131改进后挖掘铲的可靠性。与原机作业效果对比，效果得到一定提高。证明挖掘铲优化设计合理，能够改善花生收获机的作业效果。

### INTRODUCTION

Peanut is one of China's important economic and oilseed crops (Wang et al., 2021; Li et al., 2018; Wang et al., 2017). In recent years, peanut planting area is increasingly expanding. The consequent problem faced has been the harvesting of peanuts, so there is a need to further improve the machine harvesting rate of peanuts (Chen et al., 2017; Shang et al., 2008). As the basic link of peanut harvester, excavating device has a great influence on the operation quality of the harvester. As the excavation device penetrates deep into the soil, the magnitude of its resistance has an essential effect on the power loss (Shi et al., 2015; Zhang et al., 2015; Wang et al., 2010; Chen et al., 2005).

The excavation device is one of the key technologies to reduce the leakage rate and is also an important measure to reduce the resistance, increase the soil breakage rate and reduce the loss. In recent years, to realize the reduction of resistance and consumption in the excavation device of harvesters, scholars at national level and abroad have conducted more research on the excavation device of root crops and solved the problem from several aspects of research and analysis (Hou et al., 2021). Kang et al. conducted experimental tests on vibratory excavation shovels and found that the increase in vibration frequency and decrease in amplitude facilitated the improvement of excavation performance and also facilitated the separation of soil from the shovel surface.

Natenadze designed a vibrating shovel to improve the effectiveness of digging in hard soils. The relation between the technology and the design parameters of the vibration excavation shovel is analysed theoretically, and the parameters are optimized (Natenadze, 2020). Wang et al. designed an ultrasonic vibration soil cutting and digging device (Wang et al., 2020). The test verified that the device could achieve resistance reduction but could not reduce machine energy consumption. Zhang C et al designed a wedge-shaped self-lubricating deep loose shovel (Zhang et al., 2021). Self-lubricating inlaid pastes were installed on the wedge-shaped sides of the handle and tip to reduce the friction coefficient on the contact surface with the soil and reduce the tillage resistance. This device consumed considerable power and had low working reliability. The excavation and gripping device of the peanut combine harvester has a compact structure. It is difficult to reduce the drag of the excavation device by adding a vibration mechanism or other devices. Therefore, it is necessary to optimize the parameters of the digging shovel to achieve the best operation effect.

In this paper, the main parameters of the peanut digging shovel are studied and analysed by conducting a kinetic analysis of the shovel. The operation process of the excavation shovel was simulated and analysed using EDEM software. After the improvement of the excavation device, the optimal working parameters of the excavation shovel were determined through tests. The results of the field trials verified the reliability of the improved digging device. The content of the study can provide a theoretical basis for subsequent research on peanut digging shovels.

## MATERIALS AND METHODS

### *Analysis of shovel resistance under ideal conditions*

From the crop's point of view, the digging device has a root shovelling as well as lifting effect on the peanut plant. From the soil's point of view, the excavation process has actually a cutting action on the soil. Without considering the physical and mechanical properties of soil, the mechanical analysis of the excavating shovel, soil and peanut was carried out. The mechanical model is relatively simple due to the lack of research on the complex properties of the soil. The forces include the resistance  $f_1$  to the movement of the soil-peanut agglomerates along the shovel surface and the edge cutting resistance  $f_2$  of the digging shovel. Therefore, in the ideal state, the resistance model of the excavation shovel is:

$$f = f_1 + f_2 = mg \tan(\alpha + \varphi) + k_r A \quad (1)$$

where:

$m$  indicates the mass of peanut-fruit-soil mixture, (kg);  $g$  denotes the gravitational acceleration, ( $m/s^2$ );  $\alpha$  denotes the angle of inclination of the shovel surface, ( $^\circ$ );  $\varphi$  indicates the angle of friction between the peanut-soil mixture and the digging shovel;  $k_r$  denotes excavation specific resistance, ( $N/m^2$ );  $A$  denotes the cross-sectional area of the soil on the surface of the excavation shovel, ( $m^2$ ).

It can be seen that, under ideal conditions, the shovel face inclination and soil conditions are the key factors affecting the digging resistance. The greater the inclination of the shovel surface, the easier it is for the digging shovel to enter the soil. However, the total resistance of excavation also increases with the increase of angle, so it is necessary to design the shovel face inclination angle reasonably. Excavation resistance and soil are closely related. Sandy loam plots with high water content have correspondingly low shear resistance and labour-saving excavation.

### *Analysis of factors influencing excavation resistance*

As shown in Fig 1(a), In order to obtain the expression of the traction force on the excavation shovel, each force acting on the excavation shovel is decomposed along the horizontal direction. The balanced equation can be written as:

$$F_1 = N_0 \sin \alpha + \mu N_0 \cos \alpha + C_a S \cos \alpha + kb \cos \alpha \quad (2)$$

where:

$F$  indicates the digging resistance, (N);  $F_1$  denotes the traction force, (N);  $k$  indicates the cutting resistance of the soil per unit width, (N/m);  $b$  indicates the width of the excavation shovel, (m);  $\alpha$  denotes the tilt angle of the shovel surface, ( $^\circ$ );  $N_0$  denotes the normal load on the excavation shovel surface, (N);  $C_a$  indicates the soil adhesion parameter;  $S$  denotes the area of the shovel surface of the excavator, ( $m^2$ );  $\mu$  denotes the coefficient of friction between the peanut and fruit soil agglomerates and the shovel surface.

The soil of the peanut planting site is uniform in texture and does not cause the dulling of the shovel blade of the excavation shovel, so the cutting resistance of the soil is negligible (Deng et al., 2014).

According to Newton's second law, the expression for the resistance of a digging shovel can be derived as:

$$F = F_1 - kb \cos \alpha = N_0 \sin \alpha + \mu N_0 \cos \alpha + C_a S \cos \alpha \tag{3}$$

As shown in Fig 1(b), mechanical analysis was carried out on excavated objects (soil, peanuts, etc.) from the shovel surface.

The mechanical equations in the horizontal and vertical directions were established.

$$\begin{cases} C_a S \cos \alpha + N_0 (\mu \cos \alpha + \sin \alpha) - N_1 (\sin \beta + \mu_1 \cos \beta) - (CS_1 + F_b) \cos \beta = 0 \\ G + C_a \sin \alpha + N_0 (\mu \sin \alpha + \cos \alpha) - N_1 (\cos \beta + \mu_1 \sin \beta) + (CS_1 + F_b) \sin \beta = 0 \end{cases} \tag{4}$$

where:

$N_1$  denotes the normal load on the excavation shovel surface, (N);  $G$  indicates the gravity of the fruit and soil mixture on the excavation shovel, (N);  $\beta$  indicates the inclination angle of the front failure surface, ( $^\circ$ );  $S_1$  denotes the area of the front shear failure surface, ( $m^2$ );  $F_b$  denotes the inertial force of the excavated object, (N);  $\mu_1$  denotes the soil-to-soil friction coefficient.

Combining Eq. 3 and Eq. 4, the mechanical model expression for the excavation resistance is obtained after simplification.

$$F = \frac{G}{Z} + \frac{CS_1 + F_b}{Z(\sin \beta + \mu_1 \cos \beta)} + \frac{C_a S}{Z(\sin \alpha + \mu_1 \cos \beta)} \tag{5}$$

Of which:

$$Z = \left( \frac{\cos \alpha - \mu \sin \alpha}{\sin \alpha + \mu \cos \alpha} + \frac{\cos \beta - \mu_1 \sin \beta}{\sin \beta + \mu_1 \cos \beta} \right) \tag{6}$$

A schematic diagram of the geometric relations established for each parameter of the excavation system is shown in Fig 1(c).

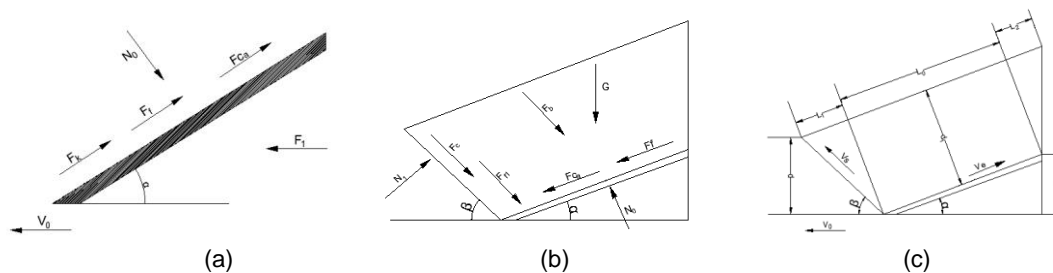


Fig. 1 - Mechanical and geometrical parameters of excavation device analysis diagram

The expressions for the gravity of the excavated object  $G$ , the inertial force of the excavated object  $F_b$ , and the area of the shovel surface  $S_1$  can be derived from the analysis as follows:

$$\begin{cases} G = \rho g b d \frac{\sin(\alpha + \beta)}{\sin \alpha} \left( L + \frac{d \cos \beta}{2 \sin \beta \cos \alpha} \right) \\ S_1 = \frac{b d}{\sin \beta} \\ F_b = \rho b d v_0^2 \frac{\sin \alpha}{\sin(\alpha + \beta)} \end{cases} \tag{7}$$

In summary, the working resistance of the excavation shovel is closely related to the physical and mechanical properties of the soil and the structural parameters of the excavation shovel, to provide a theoretical basis for the selection of subsequent test factors for the optimization of excavator structure parameters.

## Design of the main parameters of the excavation shovel

### Design of shovel face inclination

When the machine works forward, the force of the object on the shovel is shown in Fig 2.

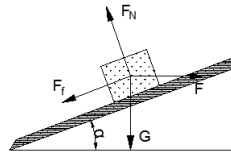


Fig. 2 - Shovel surface force analysis

Through the mechanical model, the following equation is established:

$$\begin{cases} F \cos \alpha - F_f - G \sin \alpha = 0 \\ F_N - G \cos \alpha - F \sin \alpha = 0 \\ F_f = \mu F_N \end{cases} \quad (8)$$

where:

$F$  indicates the force required to move the excavated object along the shovel, (N);  $F_N$  denotes the reaction force of the excavation shovel on the soil, (N);  $G$  indicates the gravity of the excavated object, (N);  $F_f$  denotes the friction between the excavation shovel and the soil, (N);  $\mu$  denotes the coefficient of friction of the soil on the excavation shovel, (N);  $\alpha$  indicates the tilt angle of the shovel surface, ( $^\circ$ ).

The solution gives:

$$\alpha \leq \arctan \frac{F - \mu G}{\mu F + G} \quad (9)$$

Through the theoretical analysis of excavation shovel resistance, it is necessary to ensure that the shovel surface inclination is less than the theoretical analysis value  $\alpha$ . If the shovel surface angle is set too large, it will cause an increase in digging resistance and energy consumption (Xu et al., 2022). Comprehensive consideration, the digging device shovel face inclination was set at 15 to 25  $^\circ$ .

### Digging deeper into the design

Based on the theoretical analysis of the resistance of excavating shovel, it is concluded that the force of excavating shovel is directly proportional to the excavation depth. As the excavation depth continues to increase, the resistance also rises sharply. According to the preliminary investigation and the relevant literature, the bearing depth of peanuts in the suitable harvest period is about 80~120mm. The applicability of excavating shovels needs to be improved as far as possible to ensure that the excavation operation loss rate and fruit leakage rate are the lowest. The excavation depth was determined to be 125mm ~ 145mm.

### Design of shovel face width

At present, the main peanut production areas mainly adopt the ridge planting mode, needing to determine the width of the digging shovel according to the combination of peanut planting agronomy. The mean value of the distribution range of peanut results is  $BS$ , and the deviation of its distribution is  $B_1$  (the standard distribution  $B_1$  takes the value of 54mm), and there is a certain deviation value  $B_2$  (generally takes the value of 30mm) when the machine is moving.

$$B = \frac{X + B_s + B_1 + B_2}{n} \quad (10)$$

Through literature review and preliminary investigation, combined with theoretical analysis, the width of excavating shovel is determined to be 250 ~ 300mm.

### Simulation model construction

On a micro level, excavation operations are a complex process. The theoretical analysis cannot directly analyse the excavator shovel force; the actual field experiment cannot observe the working process of

excavating shovel, and the soil movement state cannot be obtained. Therefore, the discrete element simulation method investigates the excavation shovel's operating mechanism. Analysing the interaction between the shovel and the soil provides a fundamental theoretical basis for the design of the excavation shovel.

**Soil particle model**

In the discrete element modelling of soil, spherical particles with a single diameter should not be used; otherwise, the accuracy and reliability of simulation results will be seriously affected. The actual soil particle size is measured by the test, considering that the simulation results will not be affected. The soil particle size was set to 3mm, and four soil particle models were established. Soil parameters were set as in Table 1.

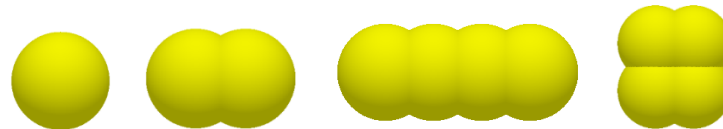


Fig. 3 - Soil particle model

Table 1

Soil parameters		
Test parameters	Unit	Numerical value
Soil Density	Kg/m <sup>3</sup>	1540
Soil Poisson's ratio	/	0.3
Soil shear modulus	Pa	1*10 <sup>8</sup>

**Excavation device model**

The excavation shovel was modelled using Solidworks software and imported into EDEM software. The material of the peanut excavation device is 65Mn steel with a density of 7810kg/m<sup>3</sup>. Its model and parameter settings are shown in Fig 4.



Fig. 4 - Excavation device model and parameter setting

**Peanut Monopoly Model**

According to the actual investigation, the ridge top width and bottom width of peanut were set as 450mm and 600mm, respectively. The model length was set to 1500 mm to reduce the simulation time. The peanut monopoly was modelled using Solidworks and then imported into EDEM software. Based on field conditions and existing soil particle simulation studies, the Hertz-Mindlin with Bonding model has less influence on the interaction between soil particles and was selected as the soil interparticle contact model (Hang et al., 2017; Horabik et al., 2008; Mak et al., 2012; Ucgul et al., 2014). The particle factory dynamically generates soil particles, which settle, pile up and bond to form peanut ridges. The model is shown in Fig 5 and the model contract parameters are shown in Table 2.

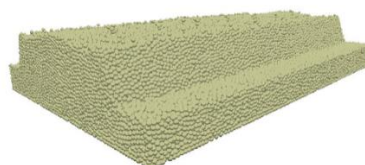


Fig. 5 - Peanut Monopoly Model

Table 2

Contact Model	Model contact parameter		
	Restitution Coefficient	Static Friction Coefficient	Rolling Friction Coefficient
Soil—Soil	0.56	0.31	0.15
Soil—65Mn	0.16	0.47	0.2

**Simulation test analysis**

To see the relation between the movement of the excavation shovel and the soil particles, three moments of the simulation process were taken to analyse the movement state of the soil, as shown in Fig 6.

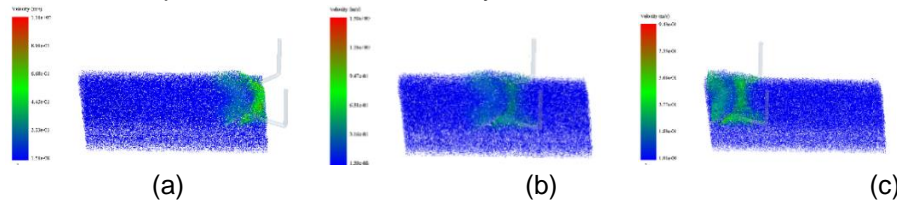


Fig. 6 - Overall view

According to the analysis of Fig 6, the different colours of the dominant bands in the graph represent soil particles of different velocities. When the digging shovel first touches the soil, the soil particles gain a certain speed and are displayed in green. However, because the shovel's contact with the ground is too small, the soil still has an overall blue state. As the digging shovel gradually enters the earth, the soil above the front of the shovel is disturbed more and more, and the speed becomes larger and larger. As the shovel surface continues to move forward, the soil particles begin to be thrown backward, at which point the velocity of the particles is increasing. When the soil is thrown to the ground, the speed becomes stationary again and starts settling.

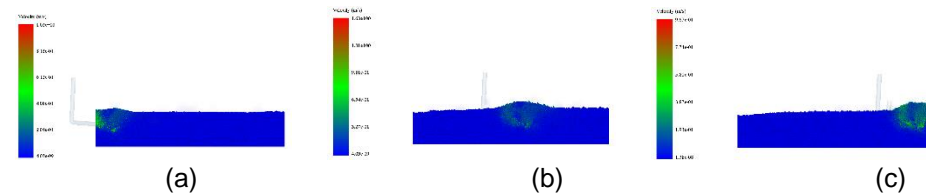


Fig. 7 - Cross-sectional view

The simulation is processed using the Clipping function to further observe the movement of the soil. It can be seen that the soil acquires a greater velocity when the tip of the excavation shovel enters the soil, indicating that the soil is more disturbed by the excavation shovel at this time. As the digging shovel undergoes movement, the direction of the velocity of the soil particles in the middle shovel surface area gradually changes to the vertical direction. This indicates that the soil starts to move upwards, which causes it to build up on the shovel surface and is an important cause of congestion. The amount of congestion then influences the change in excavation resistance.

**Influence of different operating parameters on digging resistance**

According to the existing research content of previous papers, the influence of shovel surface inclination, excavation depth, shovel surface width, and operating speed on the working resistance is studied. After Origin treatment, more intuitive resistance variation rules were explored to lay a theoretical foundation for the subsequent optimization of excavating shovel.

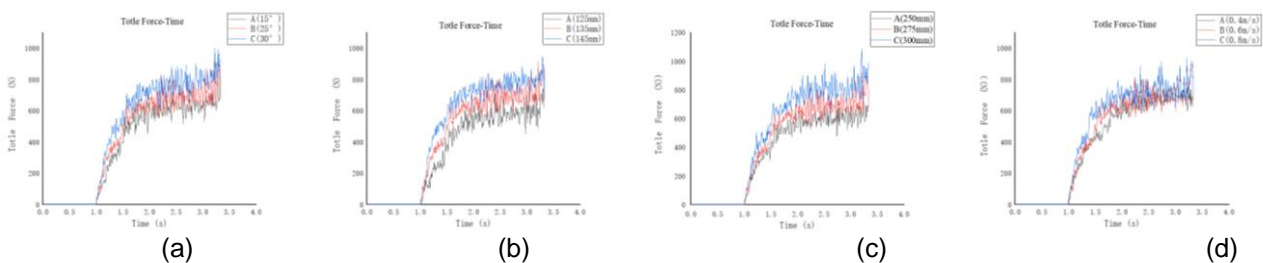


Fig. 8 - Digging resistance comparison

Figure 8 (a, b, c, d) indicates the variation law of resistance at different shovel surface inclinations, different digging depths, different shovel surface widths, and different operating speeds, respectively. Excavation resistance increases with the increase of shovel surface inclination, excavation depth, and shovel surface width, and the change of resistance is more pronounced. When the speed of the machine is changed, the resistance of the excavation is not obvious. Therefore, the effect of working speed on drag can be ignored.

**Optimization and improvement of excavation device**

Through the theoretical and simulation analysis in the previous section, the influencing factors on shovel resistance were determined, and the interaction characteristics of "shovel-soil" were analysed at the microscopic level. In order to further reduce the resistance of the excavation shovel and improve the ground-breaking effect, a Fence bar excavation shovel is designed. The high-water content of the soil results in high cohesion. Therefore, this form is used to destroy the cohesion between the soils, further break the soil and reduce the adhesion of the soil to the shovel surface. In order to ensure that the peanut-soil through the bump on the crushing soil effect is better, the fence bar spacing is set to 20mm. Its structure is shown in Fig. 9.

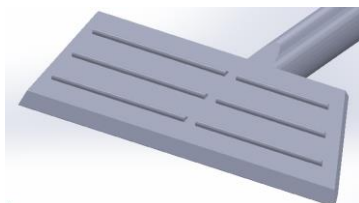


Fig. 9 - Grate excavation shovel

**RESULTS**

**Test comparison of excavation device before and after improvement**

After saving the changed excavation shovel in STL format, it was imported into EDEM for simulation test. Five sets of tests were designed to compare the two excavation devices' resistance and soil breaking rate. The excavation resistance was solved for the average value based on the data plots, and the soil fragmentation rate was derived from the number of bonds before and after the test. The data is shown in Table 3.

Table 3

Comparison of test data				
Test number	Excavation resistance		Soil fragmentation rate	
	Original excavation shovel	Fence bar excavation shovel	Original excavation shovel	Fence bar excavation shovel
1	724.13	652.71	52.12	62.37
2	809.25	715.94	49.34	61.24
3	715.64	649.55	53.66	64.03
4	653.71	576.35	55.91	64.91
5	824.63	734.63	50.62	61.71

By comparing the data, the improved excavation device works better than the former, which proves the practical design.

**Multi-factor test**

The problem of resistance to the excavation shovel and the damaging effect on the soil were investigated. The test factors are the shovel surface inclination, digging depth, and width. Excavation resistance and soil fragmentation rate were selected as test indicators. Box-Behnken tests were conducted using the response surface method, and each set of tests was repeated three times to determine the best combination of parameters for the excavation device. The test factors and codes are shown in Table 4.

Table 4

Experimental factors and levels			
Factor level	-1	0	1
Shovel face inclination	15	20	25
Digging Deeper	125	135	145
Width of shovel surface	250	275	300

The experimental design scheme and results are shown in Table 5.

Table 5

Test plan and results					
Serial number	X <sub>1</sub>	X <sub>2</sub>	X <sub>3</sub>	Y <sub>1</sub>	Y <sub>2</sub>
	Shovel face inclination	Digging Deeper	Width of shovel surface	Excavation resistance	Soil fragmentation rate
	°	mm	mm	%	%
1	20	135	275	673	64.62
2	20	125	300	673	63.91
3	25	135	300	761	64.01
4	20	135	275	675	64.51
5	15	125	275	607	62.15
6	15	135	250	600	62.17
7	15	135	300	692	63.52
8	20	145	250	722	62.39
9	25	145	275	790	63.62
10	20	135	275	661	64.13
11	20	135	275	664	64.43
12	20	145	300	815	64.23
13	20	125	250	603	62.11
14	15	145	275	716	62.56
15	25	135	250	646	63.07
16	20	135	275	668	64.46
17	25	125	275	671	63.41

### Regression analysis and significance test

Based on the experimental protocol and results, the data was analysed by multiple regression fitting using Design-Expert 13 software. A full-factor coded mathematical regression model was established with shovel surface inclination, excavation depth, and shovel face width as independent variables and excavation shovel resistance and soil fragmentation rate as objective functions.

(1) Excavation resistance response surface regression model:

$$Y_1 = 668.2 + 31.63X_1 + 61.13X_2 + 46.25X_3 + 2.5X_1X_2 + 5.75X_1X_3 + 5.75X_2X_3 - 0.35X_1^2 + 28.15X_2^2 + 6.9X_3^2 \quad (11)$$

(2) Soil fragmentation rate response surface regression model:

$$Y_2 = 64.43 + 0.46X_1 + 0.15X_2 + 0.74X_3 - 0.05X_1X_2 - 0.1X_1X_3 - 0.01X_2X_3 - 0.73X_1^2 - 0.76X_2^2 - 0.51X_3^2 \quad (12)$$

Analysis of variance and significance tests were performed on the established response surface regression models. The regression model ANOVAs for excavation shovel resistance and soil fragmentation rate is shown in Table 6 and Table 7.

Table 6

Analysis of variance for mining resistance				
Sources	Squares	DF	MS	F value
<b>Model 1</b>	48091.79	9	83.04	< 0.0001
X <sub>1</sub>	6786.13	1	105.46	< 0.0001
X <sub>2</sub>	24420.50	1	379.49	< 0.0001
X <sub>3</sub>	13530.13	1	210.26	< 0.0001
X <sub>1</sub> X <sub>2</sub>	72.25	1	1.12	0.3245
X <sub>1</sub> X <sub>3</sub>	100.00	1	1.55	0.2526
X <sub>2</sub> X <sub>3</sub>	110.25	1	1.71	0.2319
X <sub>1</sub> <sup>2</sup>	2.69	1	0.0419	0.8437
X <sub>2</sub> <sup>2</sup>	2857.27	1	44.40	0.0003
X <sub>3</sub> <sup>2</sup>	118.27	1	1.84	0.2173
<b>Residual</b>	450.45	7		
<b>Lack of Fit</b>	345.25	3	4.38	0.0939
<b>Pure Error</b>	105.20	4	R <sup>2</sup>	0.9907
<b>Cor Total</b>	48542.24	16	Adj R <sup>2</sup>	0.9788

Note: highly significant ( $P < 0.01$ ); significant ( $P < 0.05$ ).

According to the analysis of Table 5, the P of this model is less than 0.001, and the value of the misfit term is more than 0.05, indicating that the established model has a high degree of fit. The coefficient of determination was 0.9907, showing only 0.0193 variations, and the predicted value error of the model was close to the field experiment value. The experimental factors in the table significantly influence the equation, and the model can be used for parameter optimization of the excavation unit.

Table 7

Soil fragmentation rate analysis of variance				
Sources	Squares	DF	MS	F value
<b>Model 2</b>	12.79	9	21.20	0.0003
<b>X<sub>1</sub></b>	1.72	1	25.66	0.0015
<b>X<sub>2</sub></b>	0.1861	1	2.77	0.1397
<b>X<sub>3</sub></b>	4.40	1	65.55	< 0.0001
<b>X<sub>1</sub>X<sub>2</sub></b>	0.0100	1	0.1491	0.7108
<b>X<sub>1</sub>X<sub>3</sub></b>	0.0420	1	0.6267	0.4545
<b>X<sub>2</sub>X<sub>3</sub></b>	0.0004	1	0.0060	0.9406
<b>X<sub>1</sub><sup>2</sup></b>	2.25	1	33.58	0.0007
<b>X<sub>2</sub><sup>2</sup></b>	2.46	1	36.63	0.0005
<b>X<sub>3</sub><sup>2</sup></b>	1.08	1	16.09	0.0051
<b>Residual</b>	0.4694	7		
<b>Lack of Fit</b>	0.3360	3	3.36	0.1362
<b>Pure Error</b>	0.1334	4	R2	0.9646
<b>Cor Total</b>	13.26	16	Adj R2	0.9191

Note: highly significant ( $P < 0.01$ ); significant ( $P < 0.05$ ).

According to the analysis of Table 6, the P of the model is less than 0.001, and the value of the misfit term is more than 0.05, indicating that the established model has a high degree of fit. The test factors significantly affect the equation, and the order of influence of the three parameters on the soil crushing impact is: shovel face inclination > shovel face width > excavation depth. The model can be used for parameter optimization of the excavation unit.

**Response surface analysis**

The data was processed using Design-Expert 13 software to obtain the response surfaces of factor interactions on excavation resistance and soil fragmentation rate.

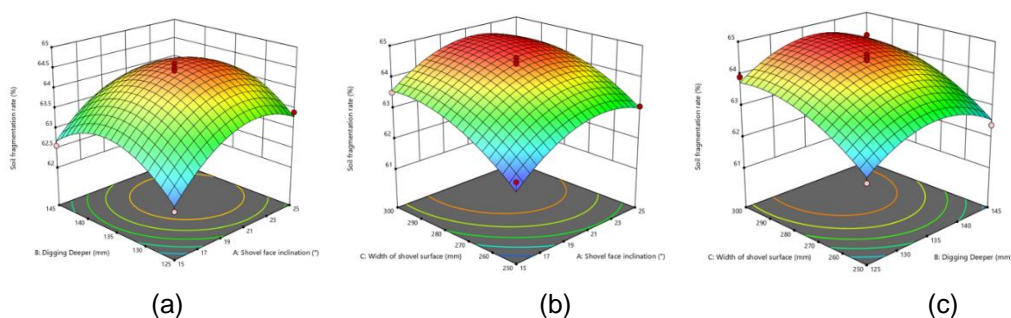


Fig. 10 - Response surface of the effect of factor interactions on excavation resistance

From Fig 10(a), it can be seen that the width of the shovel face remains the same. The digging depth is 125~135mm, and the digging resistance increases sharply after a slow increase. The digging resistance rises steadily with the shovel face inclination. From Fig 10(b), it can be observed that the excavation depth remains the same. With the shovel surface inclination increase and shovel face width, the digging resistance tends to rise. The width of the shovel surface influences the digging opposition. From Fig 10(c), it can be observed that the shovel face inclination angle remains constant. As the digging depth increases, the digging resistance increases slowly and then rises sharply. When the shovel surface width increases from 250mm to 300mm, the digging resistance rises steadily.

In a comprehensive analysis, the increase in shovel surface width and excavation depth leads to an increase in the weight of soil on the shovel surface. An increase in shovel surface inclination leads to a rise in congestion, leading to an increase in digging resistance. Therefore, taking as small a value as possible is essential to ensure that the digging resistance is not too high.

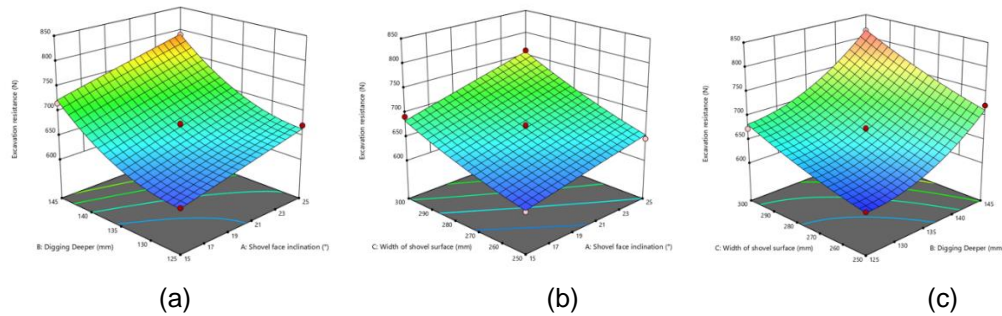


Fig. 11 - Response surface of the effect of factor interactions on soil fragmentation rate

From Fig. 11(a), it can be observed that the width of the shovel surface remains the same. With the increase of shovel surface inclination and excavation depth, the soil fragmentation rate shows a trend of increasing and decreasing. From Fig 11(b), it can be observed that the excavation depth remains the same. The soil fragmentation rate rises sharply in the range of 250~287mm at the shovel surface, after which the trend does not change significantly. Soil fragmentation rate increases with shovel surface inclination and then slightly decreases. From Fig 11(c), it can be observed that the shovel surface inclination angle remains constant. Soil fragmentation rate increases continuously with the width of the shovel surface and increases and then decreases with the excavation depth. Comprehensive analysis shows that the rise in shovel surface width and shovel surface inclination increases the soil contact area and causes the soil to break up. The increased tendency of the shovel surface raises the height of dirt falling from the back end of the shovel face, making it easier to break up the soil.

**Optimization analysis of excavation device parameters**

To achieve the best operational performance of the excavation unit, the influencing index parameters need to be minimized. The two indicators are considered together, and the operating parameters are optimized in a targeted manner.

The objective function and constraints are expressed in Equation (13).

$$\begin{cases} Y_1 = F(X_1, X_2, X_3) \rightarrow \min \\ Y_2 = F(X_1, X_2, X_3) \rightarrow \max \\ s.t. \begin{cases} -1 \leq X_1 \leq 1 \\ -1 \leq X_2 \leq 1 \\ -1 \leq X_3 \leq 1 \end{cases} \end{cases} \tag{13}$$

Optimization analysis of the best combination of results was performed using Design-Expert 13. The optimal working parameters include shovel surface inclination, digging depth, and shovel surface width of 20°, 131mm, and 277mm, respectively. The digging resistance and soil fragmentation rate were 583N and 64%, respectively.

**Field trials**

The optimal operating parameters of the excavation shovel were derived after simulation tests of the excavation unit. Field trials were conducted based on the optimal operating parameters obtained from the tests to further verify the operational effectiveness of the fence bar excavation shovel.



Fig. 12 - Field trials

The test results are shown in Table 8.

Table 8

Serial number	Field trial data	
	Peanut loss rate	
	Fence bar excavation shovel	Original excavation shovel
1	1.25	1.75
2	1.09	1.62
3	1.19	2.07
4	0.97	1.85
5	1.35	1.96
<b>Average value</b>	1.17	1.85

## CONCLUSIONS

(1) In order to explore the main factors affecting the excavation resistance, a mechanical model of the excavation device was established. Through theoretical analysis, the influencing factors and their value range are determined.

(2) To further explore the excavation operation, a discrete element simulation model was constructed. The change law of excavation motion and excavation resistance is analysed by experiments.

(3) In order to obtain the optimal working parameters of the excavation shovel, the orthogonal test of three factors and three levels was carried out. Analysis of the test results yielded the best combination of operating parameters: shovel surface inclination of 20°, digging depth of 131 mm, and shovel surface width of 277 mm. Field trials were conducted under optimal operating parameters, and the results showed that the peanut loss rate was reduced by 0.68% and the improved digging shovel was reasonably designed.

## ACKNOWLEDGEMENT

This research was funded by Modern Agricultural Industrial Technology System Project (CARS-13) and Shandong Provincial Key Science and Technology Innovation Engineering Project (2021CXGC010813).

## REFERENCES

- [1] Chen Zhihua, Li Yaoming, Sun Xingzhao, (2005). Dynamic analysis and experiment of peanut excavating shovel (花生挖掘铲动力学分析与试验), *Transactions of the Society for Agricultural Machinery*, Vol.36, Issue 11, pp. 59-63.
- [2] Chen Zhongyu, Gao Lianxing, Chen Charles et al., (2017). Status and development analysis of peanut harvesting mechanization technology in China and America (中美花生收获机械化技术现状与发展分析), *Transactions of the Society for Agricultural Machinery*, Vol.48, Issue 4, pp. 1-21.
- [3] Deng Weigang, Wang Chunguang, Sun Hong et al, (2014). Construction of mechanical model of potato excavator (马铃薯挖掘机挖掘铲力学模型构建), *Agricultural Mechanization Research*, Vol.36, Issue 01, pp. 84-86.
- [4] Hang C, Gao X, Yuan M, et al. (2018). Discrete element simulations and experiments of soil disturbance as affected by the tine spacing of subsoiler. *Biosystems Engineering*, 168: 73-82.
- [5] Horabik J, Wiącek J, Parafiniuk P. et al. (2020), Calibration of discrete-element-method model parameters of bulk wheat for storage. *Biosystems Engineering*, 200: 298-314;
- [6] Hou Jialin, Chen Yanyu, Li Yuhua, et al, (2021). Design and experiment of shovel - sieve combined scallion excavating, shaking and cleaning device (铲筛组合式大葱挖掘抖土疏整装置设计与试验), *Transactions of the CSAE*, Vol.37, Issue 18, pp. 29-39.
- [7] Kang W S, Halderson J L, Goodyear J D, (1991). A two-row vibratory potato digger[J]. *Paper-American Society of Agricultural Engineers (USA)*, 1991.
- [8] Li Guanghui, Wang Xingjun, Shi Suhua, et al., (2018). Research status and prospect of fresh food peanuts in China (我国鲜食花生研究现状及展望), *Chinese Journal of Oil Crops*, Vol.40, Issue 4, pp.604-607.
- [9] Mak J, Chen Y, Sadek M A, (2012). Determining parameters of a discrete element model for soil-tool interaction[J]. *Soil&Tillage Research*, Vol.118:117-122.
- [10] Natenadze N. The design and theoretical justification of a vibratory digger shovel[J]. *Mechanization in agriculture & Conserving of the resources*, 2016, 62(1): 9-11.

- [11] Shang Shuqi, Zhou Yalong, Wang Xiaoyan, et al., (2008). Comparative experimental study on operating performance of three peanut harvesters (三种花生收获机的作业性能对比试验研究). *Transactions of the CSAE*, Vol.24, Issue 6, pp. 150-153.
- [12] Shi Chao, Yang Ranbing, Shang Shuqi, (2015). Finite element statics analysis of peanut harvester excavating device based on UG (基于UG的花生收获机挖掘装置有限元静力学分析), *Agricultural mechanization Research*, Vol.37, Issue 1, pp. 18-21.
- [13] Ucgul M, John M F, Chris S, (2014). 3D DEM tillage simulation: validation of a hysteretic spring (plastic) contact model for a sweep tool operation in a cohesionless soil[J]. *Soil&Tillage Research*, Vol.144:220-227.
- [14] Wang Bokai, Yu Zhaoyang, Hu Zhichao, et al., (2021). Numerical simulation and experiment of the flow field of the three-air air separation system of peanut picker (花生捡拾收获机三风系风选系统流场数值模拟与试验), *Transactions of the Society for Agricultural Machinery*, Vol. 52, Issue 11, pp. 103-114.
- [15] Wang Bing, Hu Zhichao, Peng Baoliang, et al., (2017). Optimization of operation parameters of spring finger screen structure of peanut combined harvester with half feeding four rows (半喂入四行花生联合收获机弹指筛结构运行参数优化), *Transactions of the CSAE*, Vol.33, Issue 21, pp. 20-28, Nanjing/ P.R.C;
- [16] Wang Dongwei, Wang Jiasheng, (2020). Design and test of soil cutting and excavating device based on ultrasonic vibration (基于超声振动的土壤切削挖掘装置设计与试验), *Transactions of the Society for Agricultural Machinery*, Vol.51, Issue 11, pp. 85-92.
- [17] Wang Hongli, Zhang Wei, (2010). Finite element analysis of deep loose shovel based on Pro E and ANSYS (基于Pro E和ANSYS的深松铲有限元分析), *Agricultural Mechanization Research*, Vol.32, Issue 12, pp. 33-36.
- [18] Xu Xing, Chen Shiguo, Hu Lihua, (2022). Design and Analysis of Excavation Mechanism of Prince Ginseng Harvester (太子参收获机挖掘机构设计及分析), *Chinese Journal of Agricultural Mechanization*, Vol.43, Issue 08, pp. 32-39.
- [19] Zhang Chong, Fan Xuhui, Wang Huze, et al, (2021). Structural design and drag reduction test of wedge-shaped self - lubricated deep loose shovel (楔形自润滑深松铲的结构设计与减阻试验), *Agricultural Mechanization Research*, Vol.43, Issue 02, pp. 78-83.
- [20] Zhang Hai-Liang, Zhao Feng-qin, (2015). Static analysis of excavating shovel based on ANSYS (基于ANSYS的挖掘铲静力分析), *Agricultural technology and equipment*, Vol.5, 55 pp. 13-15.